biophysical chemists, but it does have a niche to fill. Any potential (or current) EXAFS practitioners must be aware of both the strengths *and* the limitations of the technique. It is hoped that this chapter has made some small contribution toward a more rational use of the EXAFS technique in the study of biological systems.

[24] Velocity Sedimentation Study of Ligand-Induced Protein Self-Association

By GEORGE C. NA and SERGE N. TIMASHEFF

A large number of protein reactions are regulated through the reversible stoichiometric interactions with small molecules or ligands. Within this wide spectrum of protein reactions, the reversible association and dissociation of protein subunits have drawn considerable research interest. The biological significance of such interactions is evident. Subunit associations are ubiquitous in key enzymes regulating metabolic pathways, in the formation of cellular organelles, and in regulatory and transporting proteins.

This chapter is devoted to the methodology of studying ligand-induced protein self-associations using the velocity sedimentation technique. The type of study described here is aimed at characterizing macromolecular associations in terms of their stoichiometries and equilibrium constants, as well as at elucidating ligand bindings to macromolecules and the equilibrium linkages between the ligand binding and the self-association reactions. The discussion is restricted to fast and reversible self-association systems. Special emphasis is given to the experimental considerations and the methods of data analysis. Theoretical treatments are minimized and limited to providing a basic conceptual framework for the data analysis. There have been several excellent articles in previous volumes of this series and elsewhere dealing with similar subjects.[1-3] The readers should consult them for references.

This chapter is divided into four sections. The first section consists of a general consideration of the experimental approach in the velocity sedimentation of ligand-induced self-association system. The second section

describes preliminary diagnoses of a ligand-induced self-association using velocity sedimentation. It can be used by those whose interest is limited to a qualitative understanding of a ligand-induced self-association system. The third section of the chapter deals with more quantitative and in-depth analyses of the velocity sedimentation data including model fitting. The last section details linked function analyses of the association systems. The methods described throughout the chapter are derived from our experience on a number of self-association systems, particularly the self-associations of the microtubule protein tubulin, which are used as examples throughout the chapter. The methods, however, should be generally applicable to other systems within the confinements of a fast, reversible self-association.

The ligand-induced dissociations of proteins into their subunits, although as interesting as the ligand-induced association, are not discussed in the present chapter. As far as the experimental approach and data analysis are concerned, they should be quite similar to the ligand-induced self-associations. One should be able to analyze such systems by making minor modifications of what is described in this chapter.

Velocity Sedimentation

Numerous review articles have been published dealing with both the theoretical and experimental aspects of velocity sedimentation. To avoid redundancy, only a few points which are less frequently mentioned and are immediately pertinent to ligand-induced self-association systems will be emphasized here.

Advantages and Limitations of Velocity Sedimentation

Many physical techniques are available for probing protein self-association. The choice of velocity sedimentation is based on its advantages, namely, that it can generate a wealth of information on the association stoichiometry and equilibrium constant through a few experimental runs and within a short time span. The shapes of the velocity sedimentation boundaries of a ligand-induced self-association are frequently diagnostic of the ligand–protein affinity. The short duration of a velocity sedimentation experiment often makes it the best choice for unstable proteins which will deteriorate if long hours of study are needed. On the other hand, it is true that the data analysis, and thus the conclusions derived from velocity sedimentation, are usually not as rigorous as for some of the other available techniques, for instance equilibrium ultracentrifugation. This, as will

become evident in the latter part of this chapter, is due mostly to the fact that in addition to the molecular weight, the size and shape of a macromolecule affect its hydrodynamic properties and, thus, both influence the sedimentation velocity of the macromolecule. This drawback sometimes can turn into an advantage when information on the size and shape of the macromolecule is desired. Notwithstanding these considerations, the ease of the experiment makes it a good choice as a preliminary probe of a system before more rigorous and time-consuming studies are undertaken.

The magnitude of the association constant measurable by velocity sedimentation is limited and these limitations should be a factor to be considered before adopting the technique. Frequently, the limiting factor is the concentration range of macromolecules that can be handled by the instrument. With schlieren optics, the protein concentration needed to obtain a usable sedimentation boundary usually lies in the range of 2 to 20 mg/ml. When using interference optics, the applicable concentration range can be extended approximately one order of magnitude at the lower end of the limit. With the optical scanner, this range depends on the extinction coefficient of the protein and it frequently can be extended down to 20–100 μg/ml.[4,5] Considering a typical protein with a molecular weight of 1×10^5, the measurable range corresponds to molar concentrations of 2×10^{-7} to 2×10^{-4} M. Since self-association reactions are best examined at or near 50% completion, this means that velocity sedimentation is suitable for measuring macromolecular interactions with association constants in the range of 5×10^3 to 5×10^6 M^{-1}, corresponding to standard free energy changes of -5 to -9 kcal/mole. The actual range is flexible to a certain extent and is dependent on the molecular weight, the association stoichiometry, and the existence of cooperativity. However, if a self-association is much stronger than the upper limit, the system will essentially behave as a nondissociating system in velocity sedimentation. Likewise, if an association is much weaker than the lower limit, it will essentially look like a nonassociating system in velocity sedimentation. These detection limits have two implications. First, experimentally, a strongly associated species frequently can be considered as nondissociating within the concentration range used in a velocity sedimentation study of its further associations. This is exemplified by the microtubule protein, tubulin. The α-β heterodimer of tubulin has an association constant of 1.25×10^6 M^{-1}.[6] Within the protein concentration ranges employed in the

velocity sedimentation studies of the magnesium and vinblastine-induced tubulin self-associations,[7-10] the dissociation of the α-β dimer is negligible. Second, one should not lose sight of the fact that the *in vivo* concentration of a given protein may not coincide with the concentration range that is suitable for velocity sedimentation study. Consequently, there will be significant self-association reactions that are not measurable by velocity sedimentation and conversely there will also be self-association reactions measurable by velocity sedimentation that are not really biologically significant.

Fast and Reversible Self-Association

As stated earlier, this chapter deals only with fast and reversible self-association systems. The velocity sedimentation of extremely slow or irreversible association systems can be interpreted in a straightforward manner and will not be discussed here. In fact, such systems frequently lend themselves better to other methods of attack, such as column gel filtration. Those systems with intermediate reaction rates, i.e., a reaction half time ranging from approximately 1 min to an hour, cannot be studied quantitatively by velocity sedimentation. It is, therefore, essential to ascertain that the reaction of interest is a fast and reversible one before proceeding with velocity sedimentation studies, as described below. The kinetics of a macromolecular association reaction are usually best determined by using a spectroscopic technique, such as the monitoring of the light scattering or fluorescence of the macromolecule. For the purpose of establishing that the reaction half time is short enough for velocity sedimentation studies, a fast-kinetic device, such as temperature jump or stopped-flow attachment, is usually not necessary. The reversibility of the reaction can be tested by determining whether the same equilibrium is reached from both the association of protomers and the dissociation of polymers. In the case of ligand-induced association systems, this can be achieved by either increasing or decreasing the solution ligand concentration, as described in the sample preparation section below.

Strong and Weak Ligand-Induced Self-Associations

In velocity sedimentation studies, ligand-induced self-association has been classified into strong ligand-induced and weak ligand-induced. The terms "strong" and "weak" used here refer to the ligand–protein affinity

and not to the protein self-association. Such classification has emerged out of the observation that ligand-induced self-associations with different ligand affinities display characteristic sedimentation boundaries and demand different experimental approaches. The affinity of the ligand in the present context is actually gauged against the total concentration of the macromolecule used. A strong ligand-induced self-association comprises systems with apparent ligand binding constants, K_x^{app}, greater than the reciprocal of the molar concentration of the macromolecule by one order of magnitude or more. Likewise, weak ligand-induced self-associations can be taken as those systems where K_x^{app} is less than the reciprocal of the molar concentration of the macromolecule by two orders of magnitude or more. Taking a macromolecule with a molecular weight of 1×10^5 at a concentration of 10 mg/ml, the reciprocal of the macromolecular concentration is $10^4\ M^{-1}$. Thus, K_x^{app} must be $10^5\ M^{-1}$ or higher to be considered a strong ligand-induced association system and $10^3\ M^{-1}$ or lower to be considered a weak ligand-induced association system. If the K_x^{app} value falls in between these two extremes, the system belongs to neither category and will be referred to as intermediate ligand-induced self-association hereon. The need for such classifications and the different experimental approaches called for, for these systems, will be detailed later.

Sample Preparation and Maintenance of a Constant Ligand Concentration

In quantitative velocity sedimentation studies of a ligand-induced self-association, the data analysis dictates that the sedimentations be carried out under a constant free ligand concentration. This is because the equilibrium constants of a ligand-induced self-association system measured by velocity sedimentation are only apparent values, due to the fact that the velocity sedimentation technique cannot differentiate between macromolecules with identical sedimentation coefficients, but with different numbers of bound ligand molecules. This can be illustrated by the simple ligand-induced dimerization reaction shown below:

$$2A + 2X \overset{k_1}{\rightleftharpoons} AX + A + X \overset{k_1}{\rightleftharpoons} 2AX \overset{k_2}{\rightleftharpoons} A_2X_2 \qquad (1)$$

where the macromolecule A binds the ligand X and two liganded macromolecules then associate to form a dimer. We adopted the convention of using lower case k's for the intrinsic or microscopic equilibrium constants and upper case K's for the apparent or macroscopic equilibrium constant. Equilibrium constants are usually expressed in units of M^{-1}. Certain calculations lend themselves better to the use of the equilibrium constants in units of ml/mg. They are denoted by the same k's or K's with the

superscript prime. k_1 and k_2 are the respective intrinsic association constants. The apparent dimerization constant of the reaction can be expressed as

$$K_2^{app} = \frac{[(AX)_2]}{([A] + [AX])^2} = \frac{k_2}{[1 + 1/(k_1[X])]^2}$$

where [X] is the concentration of the free or unbound ligand. The numerator contains all the dimer species present in the solution whereas the denominator contains all the monomer species in the solution. Assuming that the intrinsic or microscopic equilibrium constants, k_1 and k_2, remain unchanged, the apparent equilibrium constant will be dependent only on the free ligand concentration. Thus, one can maintain a constant apparent association constant only by working at a constant free ligand concentration.

For a weak ligand-induced self-association, no extra care needs to be taken to achieve a constant free ligand concentration. Since the concentration of the ligand added to the solution will be much higher than the concentration of the macromolecule, the free ligand concentration will not be significantly different from the total ligand concentration. This is exemplified by the magnesium ion-induced tubulin self-association.[7,8] Since the magnesium ion-tubulin binding constant is $10^2\ M^{-1}$, the study was carried out within the range of magnesium ion concentrations of 10^{-3} to $1.6 \times 10^{-2}\ M$. This is much higher than the protein concentration used. Consequently, the zweition was introduced into the protein solution simply by adding small aliquots of a high concentration stock solution.

For a strong or intermediate ligand-induced self-association, a constant free ligand concentration can be maintained by equilibrating the protein at a known concentration of the ligand, using a method such as gel filtration or equilibrium dialysis.[9,10] The gel filtration method is more suitable for handling proteins or ligands that are available only in small quantities. For unstable proteins, the short duration of gel filtration is also advantageous over the equilibrium dialysis method. Usually a column with dimensions of 1×10 cm, packed with a gel such as Sephadex G-25 is sufficient for equilibrating a 20-mg protein sample. To eliminate the effect of temperature variation, it is best to jacket the column and regulate its temperature by a circulating water bath. Before applying the protein, the column should be washed thoroughly with the experimental buffer containing the ligand. Small aliquots of 0.5 ml can be collected from the column and used directly in the velocity sedimentation experiments. Aliquots collected in different regions of the eluting peak usually can provide a range of protein concentrations. Since the ligand binding of such a system is dependent on the total protein concentration, once the ligand

equilibration is achieved there should be no further attempt to adjust the protein concentration by dilution with the experimental buffer, since this would release bound ligand and disturb the solution free ligand concentration. An indication of satisfactory ligand equilibration is given by the identity of sedimentation boundaries obtained from fractions in the leading edge of the eluting peak and in the trailing edge of the peak, provided that they are of the same protein concentration. Since the transport of macromolecules in a gel column is similar to that in velocity sedimentation, it is likely that depletion of free ligand at the trailing edge of the eluting peak will occur for strong ligand-induced self-associations. If, in the particular gel used, the partition coefficients of the protein species vary with the degree of polymerization, the above ligand depletion effect could be significant at low ligand concentrations. This is usually indicated by consistently different sedimentation boundaries obtained from aliquots taken at the leading edge and the trailing edge of the eluting peak, despite the fact that they are of the same protein concentration, and that efforts, such as increasing the size of the column and decreasing the rate of elution, have been made to achieve equilibration. Under such conditions, one can either use only fractions in the leading edge of the peak where ligand depletion is expected to be less severe, or switch to equilibrium dialysis for achieving the ligand–protein equilibration.

An advantage of using gel filtration or equilibrium dialysis to equilibrate the protein with the ligand is that the ligand concentration is increased gradually rather than abruptly as in the introduction of aliquots of concentrated stock solution of the ligand. Frequently, this can avoid the formation of irreversible aggregates.

Another measure which can sometimes effectively prevent the deterioration of the protein sample is to introduce the ligand to the protein solution at the earliest stage of the sample preparation. Many proteins, including allosteric enzymes, are known to be stabilized by their ligand effectors.

Selection of Optics

As mentioned earlier, the concentration range of the protein and the optics of the centrifuge to be used depend on the magnitude of the self-association constant to be determined. Schlieren optics are suitable for high protein concentrations up to 20 mg/ml, while interference optics are applicable in the concentration range below 5 mg/ml. The applicable concentration range for the optical scanner depends on the extinction coefficient of the protein at the particular wavelength used. For a wide range of coverage, more than one type of optics should be employed. The readabil-

ity of the schlieren boundaries usually deteriorates below 4 mg/ml of protein; at that point, the interference optics should take over. If the optical scanner is used in a system where the ligand of interest also absorbs light, one must choose the scanning wavelength judiciously to assure that the boundaries obtained correspond to that of the protein and not the ligand.

Calculation of the Weight-Average Sedimentation Coefficient

For rigorous quantitative analysis of velocity sedimentation data, the second moment of the sedimentation boundary should be used in the calculation of the weight-average sedimentation coefficient. This is particularly true for those strongly skewed or bimodal boundaries where the second moment could differ substantially from the apex of the boundary. Traditionally, schlieren boundaries recorded on glass plates are measured manually with a microcomparator, such as the Nikon Model-6C. To simplify the plate measurement, the manual type micrometers on the microcomparator can be replaced with an electronic type, such as the Elk Model 9200 precision digital positioner. As one turns the positioner, it sends out digital pulses which can be counted by a digital counting device. An LED then displays the digital count directly. The x-interval between two readings should depend on the sharpness of the boundary. For a boundary that spans approximately 0.5 cm on the plate, an interval of 10–20 μm per reading can be used outside the apex of the boundary and 5 μm per reading is usually sufficient around the apex. The second moment of the boundary can be calculated from these readings through numerical integration, using the trapezoidal rule:

$$\bar{r}^2 = \frac{\int_{r_m}^{r_p} r^2 \frac{dn}{dr}\, dr}{\int_{r_m}^{r_p} \frac{dn}{dr}\, dr} \cong \frac{\sum_{i=1}^{n} \left[\left(r^2 \frac{dn}{dr}\right)_{i+1} + \left(r^2 \frac{dn}{dr}\right)_i\right] \frac{r_{i+1} - r_i}{2}}{\sum_{i=1}^{n} \left[\left(\frac{dn}{dr}\right)_{i+1} + \left(\frac{dn}{dr}\right)_i\right] \frac{r_{i+1} - r_i}{2}}$$

where $\bar{r}$ is the second moment of the boundary, r is the radius, and (dn/dr) is the refractive index gradient obtained from the schlieren boundary. The integration should be carried out from a point in the supernatant to a point in the plateau. For sedimentation boundaries obtained through either interference optics or with an optical scanner, the second moment can be calculated according to

$$\bar{s} = \frac{\int_{r_m}^{r_p} r^2 dc}{\int_{r_m}^{r_p} dc} \cong \frac{\sum_{i=1}^{n} \frac{\Delta c_i}{2} (r_{i+1}^2 + r_i^2)}{\sum_{i=1}^{n} \Delta c_i}$$

where c is the weight concentration of the macromolecule. With interference optics, since the vertical distance between two fringes represents a fixed concentration increment, the measurement of the second moment can be simplified by taking the x axis readings where the hairline of the microcomparator intersects the fringes. A programmable hand calculator is sufficient for the numerical integration. However, the entire process of data acquisition and analysis can be greatly simplified if the digitized results, either from a microcomparator or directly from an electronic optical scanner, are processed directly by a computer. From the second moments of the boundaries, the weight-average sedimentation coefficients can be calculated, converted to the condition of water at 20°, and plotted against the total protein concentration. It is important to emphasize here that the weight-average sedimentation coefficient obtained is a rigorous measure of the sedimentation of the macromolecules in the plateau region.[11] This fact has two implications. First, this sedimentation coefficient is independent of the protein or ligand concentration gradient present at the boundary. Second, one should use the protein concentration at the plateau region in the above plot. If the sedimentation coefficients were obtained from boundaries that have traveled a substantial distance from the miniscus, it is prudent to take into consideration the radial dilution effect and calculate the actual protein concentration by using the average of the second moments used in calculating the sedimentation coefficient.

Qualitative Diagnosis of a Ligand-Induced Self-Association

Velocity Sedimentation in the Absence of the Ligand Effector

When confronted with a protein without any prior knowledge of its self-association properties, the initial work involves a characterization of the velocity sedimentation of the protein in the absence of the ligand effector, i.e., usually in a buffer that contains the minimum ingredients necessary to maintain the pH and the integrity of the protein. The protein under such conditions can be taken as the "ground state" of the self-association reaction. First of all, the protein ought to be examined for its

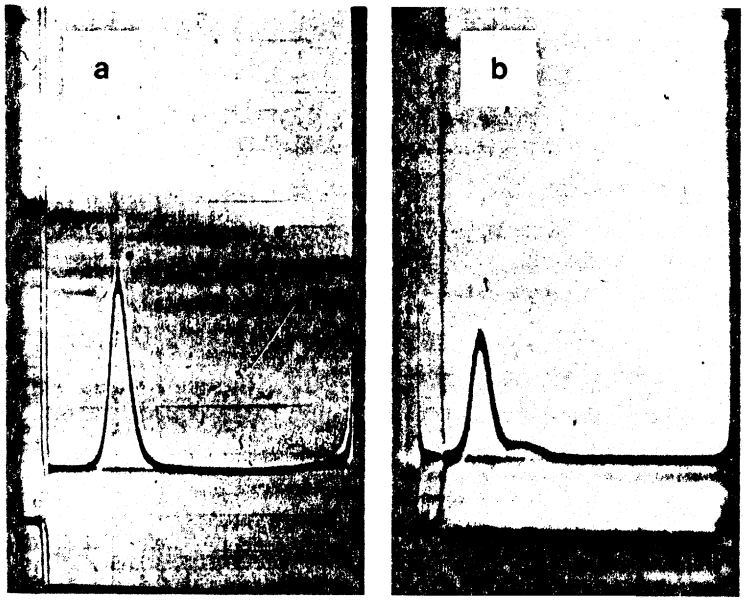

FIG. 1. Typical velocity sedimentation patterns of a homogeneous globular protein in its native state (a) and its partially, but irreversibly self-aggregated state (b). The pictures shown are those of calf brain tubulin (8 mg/ml) in 0.01 *M* NaP_i, 10^{-4} *M* GTP, pH 7.0 buffer sedimented at 60,000 rpm.

homogeneity through analysis of the shape of the sedimentation boundary. A homogeneous globular protein ought to display a single peak with its trailing edge slightly sharper than the leading edge, as exemplified by the sedimentation boundary of calf brain tubulin in a phosphate buffer shown in Fig. 1a. The sedimentation boundaries should also be closely examined both during rotor acceleration and throughout the run to assure that the protein has neither dissociated into smaller species nor aggregated irreversibly during the course of the run. The presence of higher molecular weight aggregates is usually indicated by the appearance of fast moving shoulders or spikes. This is exemplified by Fig. 1b, showing a velocity sedimentation boundary of the same protein sample as Fig. 1a, except that it had undergone a small degree of self-aggregation. Such examination is, of course, only complementary to other techniques, such as gel electrophoresis and equilibrium ultracentrifugation, which are inherently more effective in probing the homogeneity of a protein. Subsequently, the weight-average sedimentation coefficient, $s_{20,w}$, of the protein ought to be determined as a function of the total protein

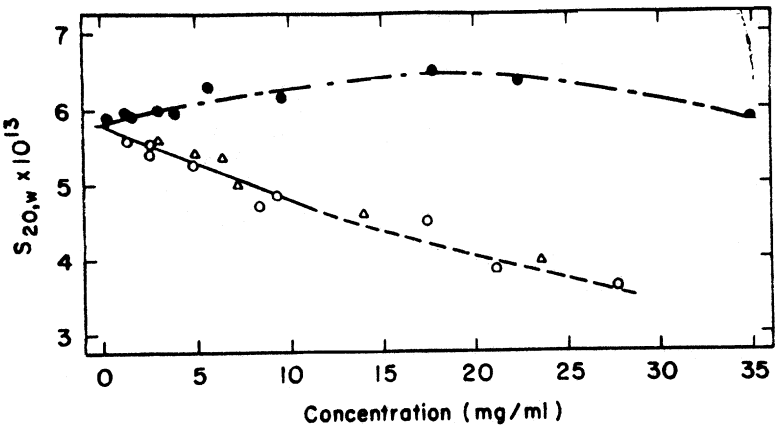

FIG. 2. Concentration dependence of the sedimentation coefficient of a globular protein under nonassociating conditions. The results shown are those of tubulin in 0.01 *M* NaP_i, 10^{-4} *M* GTP, pH 7.0 buffer. The straigth line through the data is the linear least-squares fit, whereas the dashed portion indicates deviation from linearity at high protein concentrations. The data represented by the filled circles were obtained in the same buffer with the addition of 0.1 *M* NaCl. The slight increase of the latter sedimentation coefficients with protein concentration suggested the presence of incipient self-association. (Taken from Frigon and Timasheff.[7])

concentration. For a homogeneous protein under nonassociating conditions, the sedimentation boundaries are usually symmetrical enough so that the apex of the boundary can be used in place of the second moment in the calculation of the sedimentation coefficient. The $\bar{s}_{20,w}$ can usually be fitted by the linear equation[12]

$$\bar{s}_{20,w} = \bar{s}^0_{20,w}(1 - gc_t)$$

where $\bar{s}^0_{20,w}$ is the weight-average sedimentation coefficient extrapolated to zero protein concentration, g is the hydrodynamic nonideality constant, and c_t is the total protein concentration in mg/ml. For globular proteins, the value of g usually ranges from 0.01 to 0.04 ml/mg and it increases with increasing asymmetry of the protein.[12,13] The positive value of g means that, for nonassociating proteins, $\bar{s}_{20,w}$ decreases with increasing protein concentration, and an increase of $\bar{s}_{20,w}$ with increasing protein concentration can be taken as an indication of the presence of a self-association reaction. These are exemplified by the sedimentation coefficients of calf brain tubulin in a phosphate buffer shown in Fig. 2. The

[12] H. K. Schachman, "Ultracentrifugation in Biochemistry." Academic Press, New York, 1959.

[13] J. L. Trujillo and W. C. Deal, Jr., *Biochemistry* **16**, 3098 (1977).

data below 10 mg/ml can be fitted well by Eq. (5) using a g value of 0.018 ml/mg. Introduction of 0.1 M NaCl into the buffer caused a slight increase of $\bar{s}_{20,w}$ with the protein concentration suggesting the presence of a weak self-association.

Velocity Sedimentation in the Presence of the Ligand Effector

In the past two decades, extensive studies using computer simulation technique have generated a wealth of information on the characteristic shapes of sedimentation boundaries for self-association systems with various association stoichiometries and ligand affinities.[7,9,14-23] Today, based on these computer simulation results, one can reach a qualitative diagnosis of an association system, including the macromolecular stoichiometry, the presence or absence of cooperativity in the self-association, and obtain an approximation of the ligand–protein affinity by simply analyzing the characteristic shapes of a few sedimentation boundaries. Such preliminary analysis of a self-association system is based primarily on two important features of a reaction boundary:

Asymmetry of the Boundary. As mentioned earlier in this section, a homogeneous nonassociating macromolecule should display a single peak with its trailing edge slightly sharper than the leading edge, due to the hydrodynamic nonideality.[16] Upon introduction of a ligand effector, the occurrence of protein self-association is usually reflected by the sedimentation boundary becoming asymmetrical, with its trailing edge extended. The degree of such a change usually increases with the self-association stoichiometry. Self-associations of lower stoichiometries usually display less skewed boundaries. They are exemplified by the magnesium ion-induced tubulin self-association shown in Fig. 3. At low magnesium ion concentrations, small oligomers dominate and the sedimentation boundaries are only slightly skewed with the trailing edge becoming more diffused than the leading edge. As the weight fractions of the higher polymers increase, the sedimentation boundaries become increasingly

[14] D. J. Cox, *Arch. Biochem. Biophys.* **112,** 249 (1965).
[15] D. J. Cox, *Arch. Biochem. Biophys.* **112,** 259 (1965).
[16] D. J. Cox, *Arch. Biochem. Biophys.* **119,** 230 (1967).
[17] D. J. Cox, *Arch. Biochem. Biophys.* **129,** 106 (1969).
[18] D. J. Cox, *Arch. Biochem. Biophys.* **142,** 514 (1971).
[19] D. J. Cox, *Arch. Biochem. Biophys.* **146,** 181 (1971).
[20] R. R. Holloway and D. J. Cox, *Arch. Biochem. Biophys.* **160,** 595 (1974).
[21] J. R. Cann and W. B. Goad, "Interacting Macromolecules." Academic Press, New York, 1970.
[22] J. R. Cann and W. B. Goad, *Science* **170,** 441 (1970).
[23] J. R. Cann and W. B. Goad, *Arch. Biochem. Biophys.* **153,** 603 (1972).

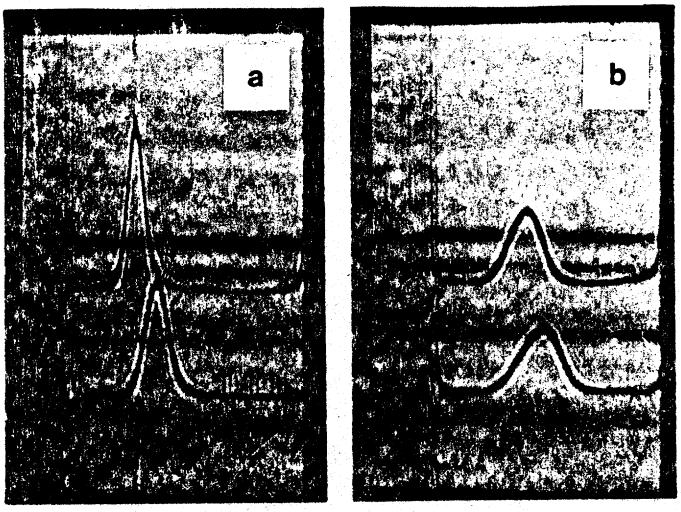

FIG. 3. Typical velocity sedimentation patterns of a weak isodesmic stepwise self-association. The results shown are those of magnesium ion-induced tubulin self-association. The speed was 60,000 rpm. The protein concentration was approximately 8 mg/ml; (a) 41 min after reaching speed; upper, no magnesium; lower, 0.0027 *M* $MgCl_2$; (b) 38 min after reaching speed; upper, 0.0055 *M* $MgCl_2$; lower, 0.0082 *M* $MgCl_2$. (Taken from Frigon and Timasheff.[7])

skewed.[20] This is also exemplified by the high concentration vinblastine-induced isodesmic indefinite self-association of tubulin shown in Fig. 4.

Modality of the Boundary. The most frequently encountered velocity sedimentation boundaries are usually either unimodal or bimodal. For a fast reversible self-association system, the bimodality of the sedimentation boundary usually indicates either the presence of cooperativity in the macromolecular self-association or the induction of the self-association by the strong binding of a ligand. The former phenomenon was first described by Gilbert[24,25] and is referred to as a Gilbert system, whereas the latter one was first reported by Cann and Goad[21-23] and is termed a Cann–Goad type sedimentation boundary.

Since a Gilbert type self-association involves some kind of cooperativity, it contains an association step or steps with a more negative free energy change than the rest of the association reaction. A moderately cooperative self-association frequently involves the formation of a looped structure as the end product. The incorporation of the last monomer to

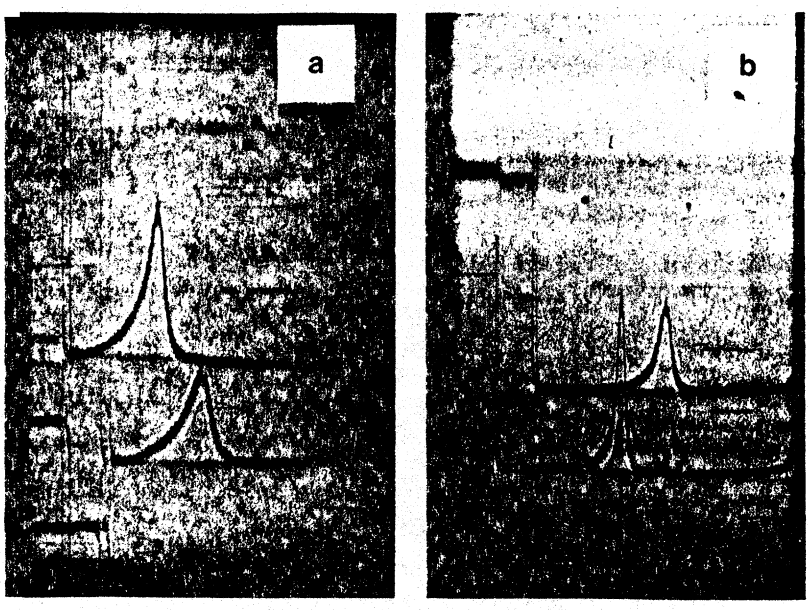

FIG. 4. Velocity sedimentation patterns of an isodesmic indefinite self-association. The results shown are those of the vinblastine-induced tubulin self-association at 60,000 rpm. The vinblastine concentrations were (a) 2×10^{-4} *M* and (b) 2.5×10^{-4} *M*. The protein concentrations were 6.7 mg/ml for the top pattern of (a), 8.3 mg/ml for the bottom pattern of (a), 8.5 mg/ml for the top pattern of (b), and 6.8 mg/ml for the bottom pattern of (b). (Taken from Na and Timasheff.[9])

enclose the looped structure is energetically more favorable because it is accompanied by the formation of two bonds instead of one.[7,8] A strongly cooperative self-association can be envisioned as resulting from multibody collisions which involves no intermediate species. In reality, the probability of such an event is small, particularly in the formation of polymers of high stoichiometries. In all likelihood, certain intermediate species do exist, but their quantities are so small they cannot be detected by existing physical techniques. In any event, the differentiation of the association pathways must rely on kinetic studies and is beyond the scope of the equilibrium studies described here. A dimerization system has only one association step which apparently would not allow the existence of any cooperativity in the self-association and it, therefore, cannot belong to a Gilbert system.

Excellent examples of the Gilbert system are provided by the tetra-

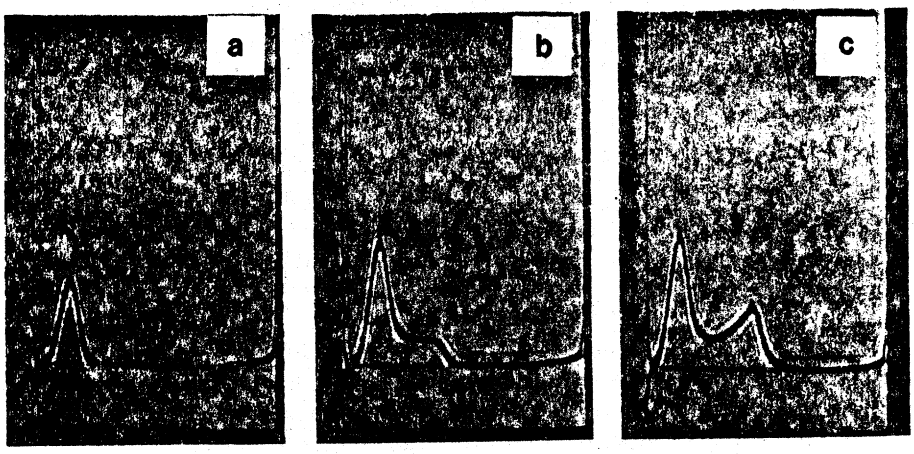

FIG. 5. Velocity sedimentation patterns of a Gilbert system. The results shown are those of magnesium ion-induced tubulin self-association to form a double ring structure of 26 ± 2-mer. The pictures were taken 21 min after reaching the speed of 48,000 rpm. The magnesium ion concentration was 0.01 *M*, whereas the protein concentrations were (a) 4.7, (b) 10.4, and (c) 15.5 mg/ml, respectively. (Taken from Frigon and Timasheff.[7])

merization of β-lactoglobulin,[26] the self-association of myosin,[27] the magnesium ion-induced self-association of tubulin into a double ring structure containing 26 ± 2 monomers[7,8] and the subunit association of phosphofructokinase.[5] In a Gilbert self-association system, as exemplified by the magnesium ion-induced tubulin self-association shown in Fig. 5, the sedimentation boundaries are unimodal at low protein concentrations, where usually stepwise isodesmically associated species predominate. Once the protein concentration is increased above a certain threshold value, the cooperative step for the formation of the favorable end product sets in and a fast moving peak begins to emerge. From there on, the size of the slow moving peak should remain constant. Further increases in protein concentration only serve to enlarge the fast moving peak. Therefore, in theory, the Gilbert system is very similar to the cooperative helical polymerization formulated by Osawa and Kasai,[28] except that in the former case the polymerization stops after the formation of the energetically favorable looped structure, whereas in the latter case the self-association continues on in a helical manner.

[26] R. Townend, R. J. Winterbottom, and S. N. Timasheff, *J. Am. Chem. Soc.* **82**, 3161 (1960).

[27] R. Josephs and W. F. Harrington, *Biochemistry* **7**, 2834 (1968).

[28] F. Oosawa and M. Kasai, *Biol. Macromol.* **5**, 261 (1971).

In the Cann–Goad systems, the bimodality of the sedimentation boundary is caused by the strong, stoichiometric ligand–protein interaction which leads to the generation of a concentration gradient of free ligand across the sedimentation boundary.[21–23] The formation of the concentration gradient can be easily understood by considering a simple asymptotic sedimentation of a ligand-induced monomer–dimer self-association system. At the beginning of the sedimentation, the monomers and dimers are in equilibrium with each other and with the free ligand. After application of a centrifugal field for a short interval, some of the macromolecules are pelleted at the bottom of the cell. For a self-associating system, the mass ratio of dimer to monomer pelleted is higher than the mass ratio of dimer to monomer found in the solution. This is simply because the dimers sediment faster than the monomers. According to the Wyman linkage theory, for a unit weight of macromolecule, more ligand is bound to the dimers than to the monomers.[29] Consequently, the molar ratio of the ligand bound to the macromolecules that pellet at the cell bottom is higher than that found in the plateau solution. This extra amount of ligand pelleted must be taken from the region centripetal to the macromolecule boundary, since in the plateau area neither the macromolecule nor the ligand changes its concentration other than as a result of radial dilution. Within the boundary, reequilibration of monomers to dimers does occur, with the binding of some free ligand. A repetition of the process, i.e., the transport of the macromolecule and the maintenance of the reaction equilibrium throughout the boundary, serves essentially as a ligand pump which constantly removes unbound ligand from the region centripetal to the boundary to the cell bottom and, thus, generates a free ligand concentration gradient across the boundary. By the same token, a similar free ligand gradient across the boundary will also be generated for a strong ligand-induced dissociation at certain intermediate ligand concentrations. However, instead of depletion, one expects to observe enhancement of the free ligand concentration centripetal to the boundary. A quantitative account of why a free ligand concentration gradient can lead to a bimodal sedimentation boundary will be given in the next section where computer simulation of the sedimentation boundary is discussed.

An excellent example of the Cann–Goad system is provided by the low concentration vinblastine-induced self-association of tubulin shown in Fig. 6. It is characteristic of the Cann–Goad system that, if the self-association is not a cooperative one, biomodal sedimentation boundaries are observed at intermediate ligand concentrations whereas unimodal sedimentation boundaries are observed at either low or high ligand con-

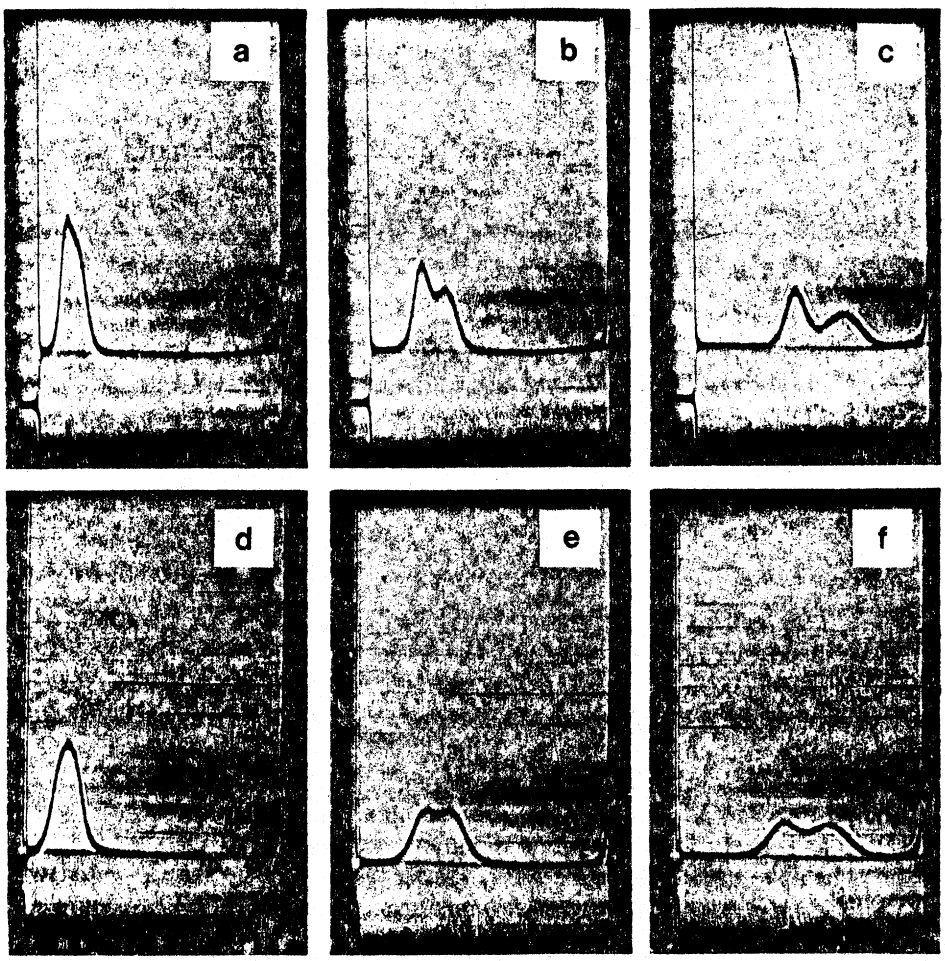

FIG. 6. Typical velocity sedimentation patterns of a Cann–Goad system. The results shown are those of tubulin in the presence of 1×10^{-5} *M* vinblastine. Pictures (a–c) were taken at 16, 32, and 64 min after reaching the speed of 60,000 rpm. Pictures (d–f) were taken from a separate run of the same sample except at 32, 64, and 104 min and at the speed of 48,000 rpm. (Taken from Na and Timasheff.[9])

centrations. Notice also that the bimodal sedimentation boundary of a Cann–Goad system first emerges from the meniscus as a single peak which then resolves into a bimodal one after sedimenting a distance from the meniscus. This contrasts with the Gilbert system where the boundary emerges from the meniscus as a bimodal one. This difference

TABLE I
MODALITY OF VELOCITY SEDIMENTATION BOUNDARIES OF VARIOUS LIGAND-INDUCED PROTEIN SELF-ASSOCIATIONS

Ligand affinity	Association	
	Isodesmic	Cooperative with favorable end-product
Weak	Unimodal	Low protein conc.: unimodal High protein conc.: biomodal (Gilbert system)
Intermediate	Low ligand conc.: unimodal	Low ligand and low or high protein concs.: unimodal
Strong	Intermediate ligand conc.: biomodal (Cann–Goad system)	High protein conc. intermediate or high ligand conc.: bimodal (trimodal?) (due to ligand gradient and/or cooperativity)
	High ligand conc.: unimodal	High protein and high ligand concs.: bimodal (due to cooperativity)

can be used to differentiate the two systems. It is also evident from Fig. 6d–f that the establishment of the Cann–Goad type bimodal sedimentation boundary is dependent on the maintenance of a stable free ligand concentration gradient across the boundary and is strongly dependent on the rotor speed. At low rotor speed, the ligand concentration gradient tends to diffuse out, leading to poorly resolved bimodal boundaries.

Table I presents a flow chart of the procedures to analyze the velocity sedimentation boundaries and to establish a qualitative characterization of a ligand-induced self-association. In carrying out the velocity sedimentation study, the most useful solution variables are the protein and ligand concentrations. In a Gilbert type cooperative self-association, at a given ligand concentration, the self-association should be examined over a range of protein concentrations. One expects to observe unimodal sedimentation boundaries at low protein concentrations and bimodal boundaries at high protein concentrations. The critical concentration at which the fast moving peak starts to emerge should decrease with increasing ligand concentration. Thus, if bimodality cannot be observed, it may be because the critical concentration is too high. One should then increase the ligand concentration in order to lower the critical concentration to

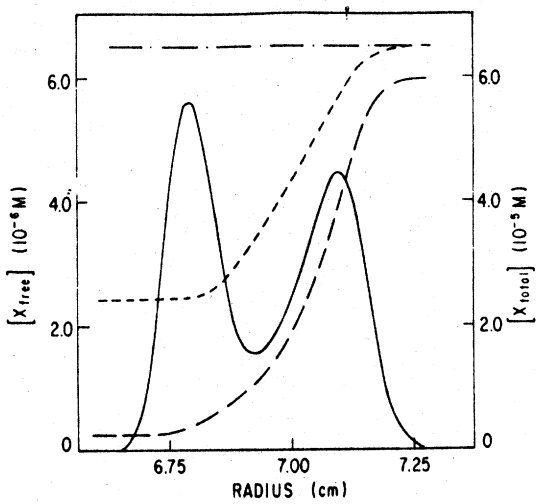

FIG. 7. Computer simulated Cann–Goad bimodal sedimentation boundary for a one-ligand-mediated monomer–dimer–trimer–tetramer isodesmic self-association. The total protein concentration was 1×10^{-4} *M*, the total ligand concentration was 6×10^{-5} *M*, and the initial free ligand concentration was 6.5×10^{-6} *M*. The microscopic equilibrium constants were 1.8×10^{4} M^{-1} for the binding of the ligand to the monomer and 1.8×10^{5} M^{-1} for the association between liganded macromolecules. The symbols are (——) protein concentration gradient, (– – –) total ligand concentration, (----) free ligand concentration, and (–·–·–) initial free ligand concentration before centrifugation (G. C. Na, J. R. Cann, and S. N. Timasheff, unpublished).

within a measurable range. A Cann–Goad type strong ligand-induced self-association can be identified by examining the sedimentation boundaries over a range of ligand concentrations. With the Cann–Goad bimodal sedimentation boundaries, if the ligand being examined has UV or visible absorption that does not overlap with the protein absorption, one should be able to use the electronic optical scanner to measure the total concentration of the ligand across the entire cell. Figure 7 depicts a computer simulated Cann–Goad type bimodal sedimentation boundary together with the distribution of the total and free ligand concentrations for a monomer–dimer–trimer–tetramer isodesmic self-association. There are two salient features to be noted. First, although the protein boundary is bimodal, the ligand boundary is only unimodal. Apparently there is little ligand bound to the protein in the slow moving peak. Second, there is a strong depletion of free ligand centripetal to the boundary. The free ligand concentration found in the supernatant is only 38% of the original free ligand concentration before the centrifugation. On the other hand, this depletion comprises only a small percentage of the total ligand concentra-

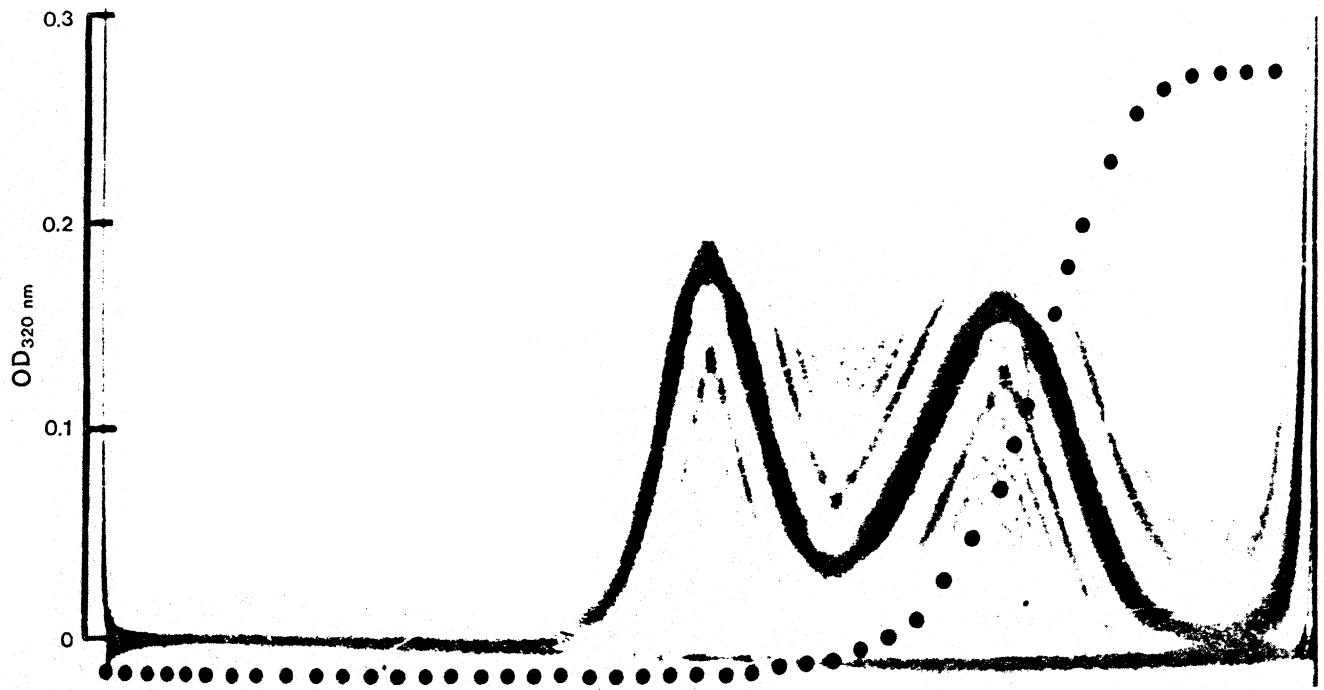

FIG. 8. Bimodal sedimentation boundary of the tubulin and vinblastine concentration distributions across the boundary. Tubulin was equilibrated with 1×10^{-5} *M* vinblastine, 0.01 *M* NaP_i, 10^{-4} *M* GTP, pH 7.0 buffer. An aliquot from the equilibrating column, containing 16.6 mg/ml tubulin, was centrifuged at 60,000 rpm in a double-sector cell with the reference sector filled with the equilibrating buffer. The schlieren picture was taken at a 65° bar angle 80 min after reaching speed. The dotted line depicts the photoelectric scan at 320 nm obtained simultaneously with the schlieren picture. (Taken from Ref. 10.)

tion in the plateau region. A simple demonstration of the presence of a total ligand concentration gradient across the boundary is apparently not sufficient evidence for a Cann–Goad system, since even a simple binding system will show such a gradient of total ligand. For a Cann–Goad system, the ligand concentration in the supernatant must be lower than the original free ligand concentration used in equilibrating the protein. These characteristics are completely born out in the bimodal sedimentation boundary of the vinblastine-induced tubulin self-association shown in Fig. 8.

By changing these solution variables and comparing the resulting boundaries with the table, one should be able to reach a preliminary diagnosis of the system of interest. Initially, in probing the effect of a particular ligand, the presence of other ligand effectors should be avoided in order to minimize complications. Other variables such as the concentration of the hydronium ion and the solution temperature should also be kept constant. After the initial characterization, one can then manipulate the latter variables to obtain information, such as the effects of different ligands and the enthalpy change of the association.

One can notice that there is a type of self-association, shown in Table I, which we are not aware of having either been encountered in a real system or having been studied theoretically. It is a cooperative self-association induced by a strong ligand binding reaction, i.e., a Cann–Goad-type Gilbert system. One would expect it to possess characteristics both of the Cann–Goad system and of the Gilbert system. It is yet uncertain whether a trimodal sedimentation boundary can emerge at certain high protein concentrations and intermediate ligand concentration. This question still awaits to be answered by computer simulation studies.

Quantitative Analysis of Ligand-Induced Self-Association

A reversible self-association system can be expressed by the following generalized equations:

$$A + A \rightleftharpoons A_2 \qquad K_2 = \frac{[A_2]}{[A]^2}$$

$$A_2 + A \rightleftharpoons A_3 \qquad K_3 = \frac{[A_3]}{[A_2][A]}$$

$$\vdots \qquad\qquad \vdots$$

$$A_{n-1} + A \rightleftharpoons A_n \qquad K_n = \frac{[A_n]}{[A_{n-1}][A]}$$

where A_n and $[A_n]$ denote the n-mer and its molar concentration. K_n's are the association constants for the formation of successive bonds between monomer and $(n-1)$-mer. For such a self-association, the mass distribution of the protein among various polymers is reflected in a functional dependence of $\overline{MW}$, the weight-average molecular weight of the macromolecule, on the total protein concentration and the association parameters:

$$\overline{MW} = \frac{\sum_{i-1}^{n} c_i MW_i}{c_t}$$

where c_i is the concentration of i-mer in mg/ml, c_t is the total protein concentration, and MW_i is the molecular weight of the i-mer. In velocity sedimentation, the mass distribution is reflected by a similar dependence of the weight-average sedimentation coefficient on the total protein concentration and the association parameters:

$$\bar{s} = \frac{\sum_{i-1}^{n} c_i s_i}{c_t} = \frac{\sum_{i-1}^{n} c_i s_i^0 (1 - g_i c_t)}{c_t}$$

where s_i and g_i are the sedimentation coefficient and hydrodynamic nonideality constant of the i-mer, respectively. Thus, by fitting the experimentally determined weight-average sedimentation coefficients with theoretical curves, calculated from various association models, one can rule out certain association schemes and determine the association stoichiometry and equilibrium constants that can describe the system best.

Another method for studying quantitatively the velocity sedimentation of a ligand-induced self-association system is through the computer simulation of the sedimentation boundaries. As mentioned earlier, the sedimentation boundaries of systems undergoing different mechanisms of association often possess strikingly different characteristics. As a result, a comparison of the experimental sedimentation boundaries with those calculated with a computer can also lead to information about the mechanism of the association reaction. These two methods of velocity sedimentation analysis are described in detail in the following section.

Probing the Association Mechanism through Analyzing $\bar{s}_{20,w}$

The selection of theoretical models to fit the experimental data is guided by the preliminary boundary analyses described previously. Further hints as to the association mechanism can be obtained from the dependence of the $\bar{s}_{20,w}$ on total protein concentration. For a stepwise self-association without any cooperative event, the weight-average sedimentation coefficient should show a simple parabolic type dependence on

total protein concentration.[9,10] On the other hand, if a cooperative step or steps are present in the self-association, a sigmoidal curve should be expected.[5,7,8] The degree of inflection of the sigmoidal curve should be directly related to the cooperativity whereas the number of inflections is related to the number of cooperative steps present. After examining the plot of $\bar{s}_{20,w}$ versus the protein concentration, preferably at several free ligand concentrations, one can set up a theoretical association model. Following the association model, the concentration of each i-mer can be calculated by numerically solving the following polynomial using the Newton–Ralphson rule:

$$c_t = \sum_{i=1}^{n} c_i = \sum_{i=1}^{n} K_2' K_3' \cdot \cdot \cdot K_i' c_1^i$$

where c_t is the total protein concentration and c_1 is the concentration of the monomer, both being in mg/ml; MW is the molecular weight of the monomer; K_i' is the apparent association constant between a monomer and an $(i - 1)$-mer in units of ml/mg. It is related to K_i in the unit of M^{-1} by the equation

$$K_i' = \frac{i}{(i - 1)\mathrm{MW}} K_i$$

It is important to recognize here that the number of self-association schemes which can be devised is limited only by one's imagination. Thus, in fitting experimental data with theoretical models, the rule to observe is to stay with the simplest model that can accommodate the data. On the practical side, the solution of Eq. (9) can be greatly simplified if one can minimize the number of variables present. In the generalized expression of a self-association system, shown in Eq. (6), each of the self-association constants can assume any value. If there is no sign of cooperativity in the self-association, one should start with a simple stepwise isodesmic self-association, i.e., one should assign the same equilibrium constant to each step of the self-association. For a moderately cooperative association system, one may assign a higher valued association constant to the cooperative step.[7,8] For a strongly cooperative system, one may even set all the intermediate association constants to zero, which is essentially equivalent to assuming the absence of all intermediate species.[5] If the self-association proceeds indefinitely and the equilibrium constants for each step of the self-association are identical, then Eq. (9) converges to a simple binomial

$$c_t = \frac{c_1}{[1 - (K_2 c_1/\mathrm{MW})]^2}$$

and the concentrations of monomer and each i-mer can be obtained easily:

$$c_i = i(K_2/\mathrm{MW})^{i-1}c_1^i$$

In the case of a cooperative self-association, both the association scheme and data analysis can be simplified substantially if it is possible to assign a single equilibrium constant for all the association steps prior to the formation of the favorable end product. The mass distributions of the protein among the various polymers for the above two association schemes can be calculated. As depicted in Fig. 9A, in the isodesmic indefinite type of self-association, the small oligomers dominate at low protein concentrations; as the concentration increases, the weight fractions of higher polymers gradually increase. Also, as shown in Fig. 9B, at a given protein concentration, if the self-associations is weak, the monomer is the dominating species and the weight fractions of the polymers decrease with

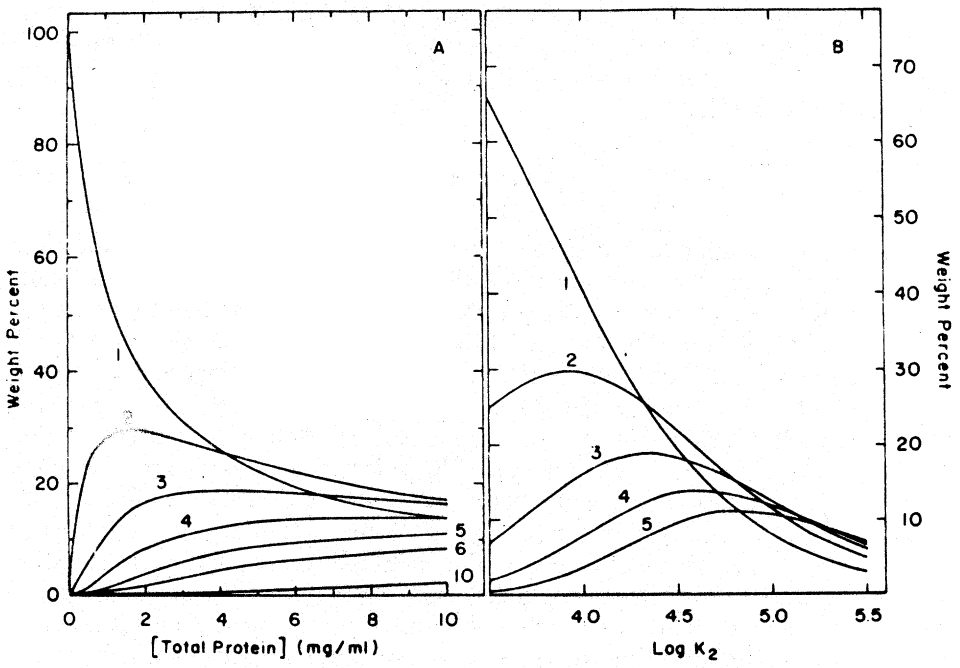

FIG. 9. Mass distribution of tubulin among different size polymers for an isodesmic, indefinite self-association. (A) Dependence on the total protein concentration; $K_2^{app} = 5.2 \times 10^4\ M^{-1}$. (B) Dependence on the polymerization constants; total protein concentration = 10 mg/ml. The number next to each curve is the corresponding degree of polymerization. (Taken from Ref. 9.)

increasing degrees of polymerization. As the association becomes stronger, the trend reverses itself, i.e., higher molecular weight species become dominant. On the other hand, for a Gilbert system, such as the magnesium ion-induced tubulin self-association shown in Fig. 10, below the critical concentration for the formation of the favorable end polymer, the weight distribution of the protein is similar to the isodesmic association described above. Above the critical concentration, the concentration of the favorable end product of the self-association, in this case a 26-mer, departs from zero and increases linearly whereas those of the intermediate species remain essentially constant.

Once the concentrations of all i-mers are obtained, they are put into Eq. (8) to calculate the theoretical weight-average sedimentation coefficient as a function of total protein concentration. The data analyses are usually carried out under the assumption that the binding of the low-molecular weight ligand does not affect the sedimentation coefficient of the macromolecule, either through a slight change of the molecular weight or a change of the structure of the macromolecule. In Eq. (8), one needs to know s_i, the sedimentation coefficient of the i-mer. In a few instances, the sedimentation coefficient of the end polymer can be derived by extrapolating the sedimentation coefficients obtained at high protein concentration and at a saturating ligand concentration. This is particularly true for the Gilbert-type strongly cooperative self-association system where a certain end polymer will dominate at high protein concentrations.[5,7,8] However, in most cases the sedimentation coefficients of individual polymers are unavailable and are not readily measureable. To pro-

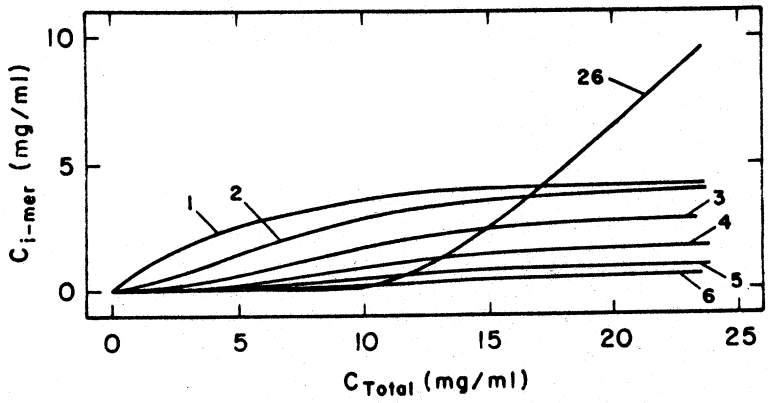

FIG. 10. Variations in the concentrations of individual species in the self-association of tubulin as a function of the total protein concentration in the presence of 0.008 M $MgCl_2$. The numbers indicate the degree of polymerization of each associated species. (Taken from Ref. 7.)

ceed with the calculation, it becomes necessary to use theoretical s_i values obtained by assuming a certain physical shape of the polymer. The simplest and most frequently used model is a spherical one for which the sedimentation coefficient of the i-mer can be calculated from

$$s_i^0 = i^{2/3} s_1^0$$

where s_i^0 is the reduced sedimentation coefficient of the i-mer and s_1^0 is the reduced sedimentation coefficient of the monomer. More complicated and elaborate models can be used, if one has some knowledge of the physical size and shape of the polymers obtained through other methods, such as electron microscopy. In this regard, study of the morphology of the polymers using an electron microscope can provide valuable information not only on the association stoichiometry but also on the size and shape of the polymer species. Examples of such an approach can be found in the magnesium-induced tubulin self-association into a double ring structure,[7,8] as well as in several other multisubunit proteins.[30,31] In some cases, the association product was observed vividly under the electron microscope permitting its sedimentation coefficient to be deduced by the Kirkwood theory.[32] The theoretical values were found to be consistent with the experimental values obtained from extrapolation.

Another unknown factor in Eq. (8) is g_i, the hydrodynamic nonideality constant of the i-mer. As mentioned earlier, the value of g appears to increase with the asymmetry of the protein. Currently, there is no solid formulation of g as a function of the size and shape of a macromolecule. The usual practice is to assign the value of g_1 to all g_i. The uncertainties in the quantities of s_i and g_i must undoubtedly lead to some errors. Such errors may stay within the experimental uncertainty for those systems where the polymers are symmetrical in shape and have low association stoichiometries, but may become significant for those systems that form asymmetrical polymers of high association stoichiometries. In the latter case, these uncertainties could prevent an unequivocal deduction of the association stoichiometry and equilibrium constant.

An association model fitting is carried out through nonlinear least-squares fitting of the experimental $\bar{s}_{20,w}$. This technique is well illustrated by the magnesium-induced formation of the tubulin double-ring structure and the vinblastine-induced isodesmic indefinite self-association of tubulin. In the magnesium-induced self-association, the sedimentation boundaries shown in Fig. 5 displayed all the characteristics of the Gilbert system described above. The weight-average sedimentation coefficients depicted

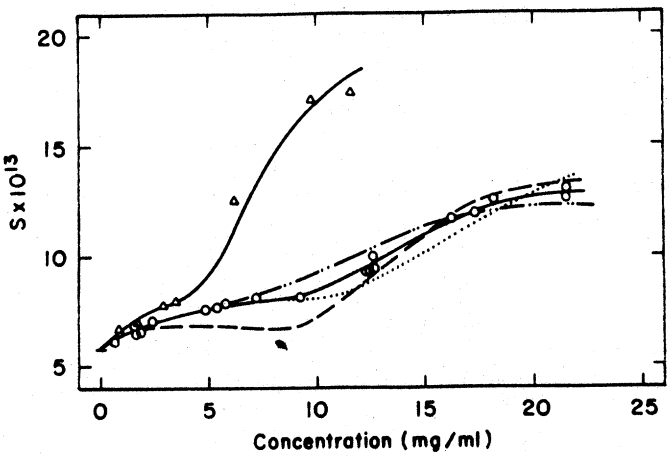

FIG. 11. Theoretical fitting of the concentration dependence of the weight-average sedimentation coefficient, $s_{20,w}$, of tubulin under self-associating conditions in the presence of Mg^{2+}. (○) 0.008 *M* $MgCl_2$; (△) 0.016 *M* $MgCl_2$. The lines are least-squares fits to the data according to the models described in Ref. 7. (Taken from Ref. 7.)

in Fig. 11 showed sigmoidal dependence on the total protein concentration and could be fitted well with an initial isodesmic self-association which then terminated at the 26-mer which formed with a more negative free energy change. In contrast, the vinblastine-induced tubulin self-association, characterized by the strongly skewed sedimentation boundaries of Fig. 6, suggested an isodesmic indefinite self-association mechanism. Further proof of the latter association mechanism was obtained from the parabolic dependence of the weight-average sedimentation coefficients on the protein concentration, as depicted in Fig. 12, and the good fit of the data by the theoretical curves calculated according to the isodesmic indefinite mechanism at various vinblastine concentrations.

Computer Simulation of Velocity Sedimentation Boundaries

The method of numerical calculation of velocity sedimentation boundaries using an asymptotic approach was first introduced by Gilbert three decades ago.[24,25] Since then, the numerical simulation technique has been greatly refined and used fruitfully in the deduction of the mechanisms of biomacromolecular self-association. Basically, there are two types of simulation methods. The first method is for those systems where no ligand gradient is formed across the boundary. They include both weak ligand-induced self-associations and strong ligand-induced self-associations at saturating ligand concentrations. With a constant ligand concentration

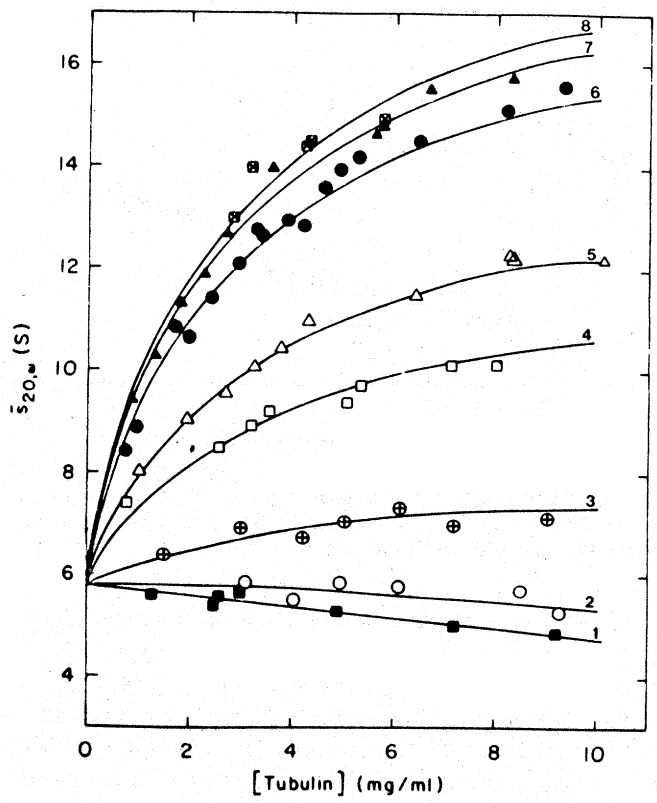

FIG. 12. Weight-average sedimentation coefficients ($\bar{s}_{20,w}$) of tubulin determined as a function of total protein concentration. Tubulin was equilibrated with different concentrations of vinblastine [(1) PG (0.01 *M* NaP_i; 10^{-4} *M* GTP, pH 7.0) only; (2) 1×10^{-6} *M*; (3) 5×10^{-6} *M*; (4) 2.5×10^{-5} *M*; (5) 5×10^{-5} *M*; (6) 1×10^{-4} *M*; (7) 2×10^{-4} *M*; (8) 5×10^{-4} *M*] in PG buffer, using both a batch and a flow column of Sephadex G-25 gel. Aliquots (0.5 ml) were collected from the column and used directly for ultracentrifugation without dilution to avoid changes in free vinblastine concentration. Solid lines are least-squares fittings of the experimental data by the isodesmic, indefinite, self-association model. (Taken from Ref. 9.)

throughout the cell, the simulation can be carried out using a constant apparent association constant. For a Cann–Goad bimodal sedimentation boundary, where a gradient of free ligand concentration does form around the boundary, the apparent association constant will vary throughout the boundary. For the latter systems, one should use the second method, which is designed to keep track of the free ligand concentration across the boundary. For those interested in carrying out the numerical simulation

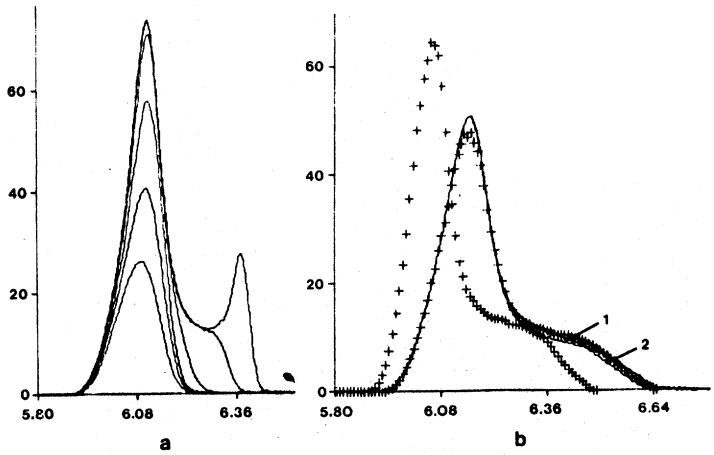

FIG. 13. Simulated sedimentation velocity profiles of magnesium-induced tubulin self-association in a sector-shaped cell at 48,000 rpm. (a) The sedimentation time was 1880 sec. A sharp initial boundary was set at 5.884 cm. The ordinate is the concentration gradient calibrated in units of mg/ml/cm and the abscissa indicates radial position in cm from the center of rotation. The protein concentrations corresponding to the shown patterns are 4.0, 6.0, 8.0, 10.0, 12.0, and 14.0 mg/ml. The association parameters are described in Ref. 7. (b) The calculated boundary was depicted by the solid curve. The experimental concentration gradient profile (+), shown at an early sedimentation time of 1260 sec was used as the initial boundary data. The theoretical profiles were then calculated for an additional sedimentation time of 720 sec and the curves are shown compared with an experimental profile (+) at 1980 sec. (Taken from Ref. 7.)

study, there have been two excellent review articles dealing with details of the methods.[33,34]

Given a theoretical self-association model, the computer simulation technique is capable of predicting boundary shapes and showing how they change in response to variations of certain molecular or association parameters. This is exemplified by Figs. 13a and 14A where, starting from synthetic hypersharp boundaries, simulated sedimentation boundaries were generated for a Gilbert system and an isodesmic indefinite self-association system. The qualitative agreement of the characteristic shapes of the simulated boundaries with the experimental boundaries found in the magnesium ion and vinblastine-induced tubulin self-associations has led to the initial confirmation of the association schemes. Fur-

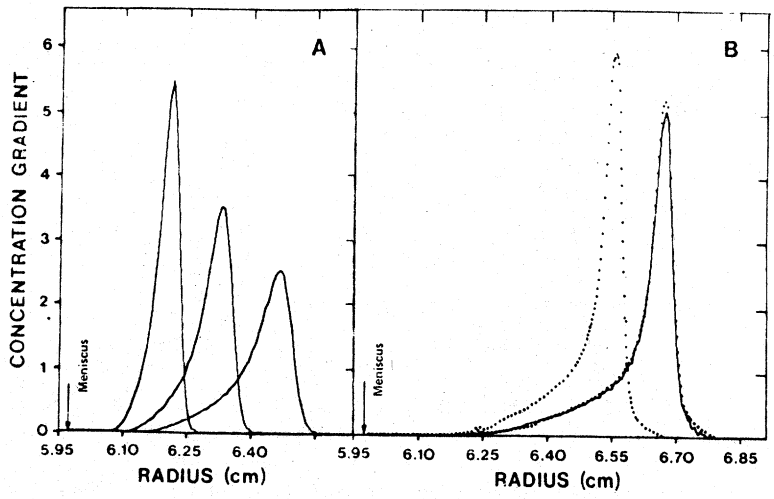

FIG. 14. Computer simulation of the velocity sedimentation profiles of tubulin in a sector-shaped cell. The ordinates for both parts A and B are in random units, whereas the abscissa represents the radial distance from the center of rotation. (A) The simulation process was started with an initial sharp boundary of 10 mg/ml set at 6.09 cm from the center of rotation. It was then subjected to simulated sedimentation at 52,000 rpm according to the isodesmic, indefinite self-association model. The resulting schlieren sedimentation patterns were calculated for 510, 964, and 1475 sec of centrifugation, respectively. (B) The simulation process was started after 32 min of sedimentation. The dotted line patterns are experimental schlieren patterns, after 32 and 40 min of sedimentation after reaching speed, of tubulin (12 mg/ml) equilibrated with 5×10^{-5} *M* vinblastine, 0.01 *M* NaP_i, 10^{-4} *M* GTP, pH 7.0 buffer. The early sedimentation pattern was used as the initial boundary for computer simulation according to the isodesmic, indefinite self-association model. The simulated sedimentation was allowed to proceed for 8 min. The resulting simulated sedimentation pattern (solid line) is to be compared with the second experimentally obtained sedimentation pattern. (Taken from Ref. 9.)

ther substantiations of the mechanisms were obtained through point-by-point comparison of the experimental boundaries with the simulated ones as shown in Figs. 13b and 14B. The latter simulations were carried out by using as the initial boundary an experimental boundary obtained from the same run at an earlier time.

The computer simulation studies, useful as they are, usually cannot generate new quantitative insights into the system other than those that have already been obtained from the analysis of the weight-average sedimentation coefficients. To begin with, in order to carry out the computer simulation, one needs to have on hand the complete functional dependence of $\bar{s}_{20,w}$ and $\bar{D}_{20,w}$ on the total protein concentration. In other words,

the analysis of the weight-average sedimentation coefficient must precede the boundary simulation. The diffusion coefficient, another unknown factor, can be measured experimentally using techniques such as light scattering. However, in practice, it is usually calculated from the weight-average sedimentation coefficient using the Svedberg equation. In the latter case, additional uncertainties will be introduced which further complicate the fitting process. If one accepts the Svedberg equation in calculating the diffusion coefficient, there should be a one-to-one correspondence between a given shape of $\bar{s}_{20,w}$ versus total protein concentration plot and a specific shape of sedimentation boundary. Several salient features of the sedimentation boundaries can be understood better if one recognizes these relationships. For instance, both the Gilbert cooperative self-association and the Cann–Goad-type strong ligand-induced self-association can give bimodal sedimentation boundaries. This is because both systems show a sigmoidal dependence of their weight-average sedimentation coefficient on total protein concentration. In the Gilbert system, the sigmoidal dependence arises from the presence of cooperativity in the self-association. In the Cann–Goad system, it arises from the generation of a concentration gradient of free ligand across the boundary. This is exemplified by the vinblastine-induced tubulin self-association, as shown in Fig. 12. At a given concentration of the free ligand, $\bar{s}_{20,w}$ increases parabolically with increasing protein concentration. However, if a concentration gradient of free ligand is present across the boundary, as shown in Fig. 7, the actual dependence of $\bar{s}_{20,w}$ on the protein concentration across the boundary will no longer follow one of the solid curves but will shift across several curves following the lower ones at low protein concentration and the higher curves at high protein concentration. If the free ligand concentration gradient is sharp, the actual dependence of $\bar{s}_{20,w}$ on protein concentration will become sigmoidal. Also, in this particular system, the self-association plateaus at saturating ligand concentrations. Thus, at a given protein concentration the increment of $\bar{s}_{20,w}$ per unit increase of ligand concentration is maximal at intermediate ligand concentrations. As a result, the actual dependence of $\bar{s}_{20,w}$ on the total protein concentration gradually loses its sigmoidal character at both high and low ligand concentrations and consequently unimodal sedimentation boundaries are observed. Furthermore, for a Cann–Goad system, since the sigmoidal dependence of $\bar{s}_{20,w}$ on the protein concentration results from the concentration gradient of the free ligand across the boundary, the sedimentation boundary first emerges as unimodal and then starts to resolve into a bimodal one only after a period of sedimentation sufficient to allow the establishment of the free ligand concentration gradient.

Probing the Multiple Equilibria of a Ligand-Induced Self-Association

In the preceding section, we demonstrated that the self-association constant of a ligand-induced self-associating system obtained from the velocity sedimentation studies is an apparent one and it is a function of the ligand activity. In this section, we will discuss the method of analyzing this function to probe the multiple equilibria of a ligand-induced protein self-association. From the multiple equilibria, one can then derive information, such as the stoichiometry and association constant of the ligand-binding site(s) linked to the self-association reaction and the mechanism through which the ligand-binding reaction brings about the self-association of the macromolecule. This method of data analysis is illustrated below by using a ligand-induced dimerization reaction as an example. Assuming that both the ligand binding and self-association reactions are fast and reversible and thus both are constantly in equilibrium, the molecular species present in the solution depends on the association pathway. Considering the following association pathways:

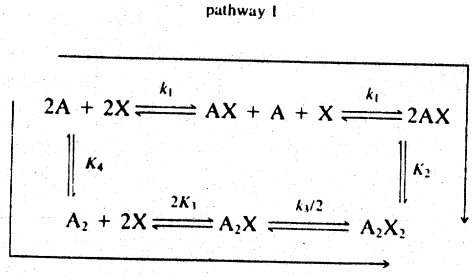

$$A + X \overset{k_1}{\rightleftharpoons} AX$$
$$AX + A \overset{k_1}{\rightleftharpoons} AXA$$
$$AX + X \overset{k_1}{\rightleftharpoons} XAX$$
$$XAX + A \overset{k_1}{\rightleftharpoons} XAXA$$
$$XAXA + X \overset{k_1}{\rightleftharpoons} XAXAX$$

where A denotes the macromolecule and X denotes the ligand, the self-associations designated as pathway I and pathway II in Eq. (14) have previously been given the names of ligand-mediated association and ligand-facilitated association, respectively.[35] In the ligand-mediated association, the ligand binding to the macromolecule precedes the self-association reaction, whereas in the ligand-facilitated association, the ligand

TABLE II

Association mechanism	K_2^{app}		$\left(\frac{\partial \ln K_2^{app}}{\partial \ln[X]}\right)_{T,P,a_{j\neq x}}$	
I	$\frac{[(AX)_2]}{([A]+[AX])^2}$	$\frac{k_2}{[1+1/(k_1[X])]^2}$	$\frac{2}{1+k_1[X]}$	
II	$\frac{[A_2]+[A_2X]+[A_2X_2]}{[A]^2}$	$k_4(1+2k_3[X]+k_3^2[X]^2)$	$\frac{2k_3[X]+2k_3^2[X]^2}{1+2k_3[X]+k_3^2[X]^2}$	
I + II	$\frac{[A_2]+[A_2X]+[A_2X_2]}{([A]+[AX])^2}$	$k_4\frac{1+2k_3[X]+k_3^2[X]^2}{(1+k_1[X])^2}$	$\frac{2k_3[X]+2k_3^2[X]^2}{1+2k_3[X]+k_3^2[X]^2}$	$-\frac{2k_1[X]}{1+k_1[X]}$
Crosslink	$\frac{[A_2X]+[A_2X_2]+[A_2X_3]}{([A]+[AX]+[AX_2])^2}$	$\frac{k_1^2[X]}{(1+k_1[X])^2}$	$\frac{1-k_1[X]}{1+k_1[X]}$	

binding follows the association reaction. If the self-association can proceed through both pathways I and II then it is called a combined ligand-mediated and facilitated mechanism. In the self-association reaction described by Eq. (15), the ligand is divalent and it serves essentially as a cross-linker between two macromonomers. This self-association mechanism will be referred to hereon as a cross-linking mechanism. For these self-association mechanisms, Table II lists the apparent dimerization constants measured by the velocity sedimentation technique, both in terms of the constituent macromolecular concentrations, and in terms of the microscopic equilibrium constants and ligand activities. Figure 15A presents plots of the logarithm of these apparent dimerization constants versus the logarithm of the free ligand concentration. This plot will be referred to as the Wyman plot, since it is essentially a reflection of the Wyman linked function[29,36].

$$\left(\frac{\partial \ln K}{\partial \ln[X]}\right)_{T,P,a_{j\neq x}} = \left(\frac{\partial m_x}{\partial m_p}\right)_{T,P,m_{j\neq p}} - \left(\frac{\partial m_x}{\partial m_r}\right)_{T,P,m_{j\neq r}}$$

$$= (\bar{X}_{product} - \bar{X}_{reactant}) - \frac{[X]}{[W]}(\bar{W}_{product} - \bar{W}_{reactant})$$

$$\cong \bar{X}_{product} - \bar{X}_{reactant} = \Delta\bar{X}$$

where m_x, m_r, m_p are the molal concentrations of the ligand, the reactant, and the product, respectively. [W] is the molal concentration of water in the solution, [X] is that of free ligand; $\bar{W}_{reactant}$ and $\bar{W}_{product}$ are the hydrations of the reactant and product, and $\bar{X}_{reactant}$ and $\bar{X}_{product}$ are the respec-

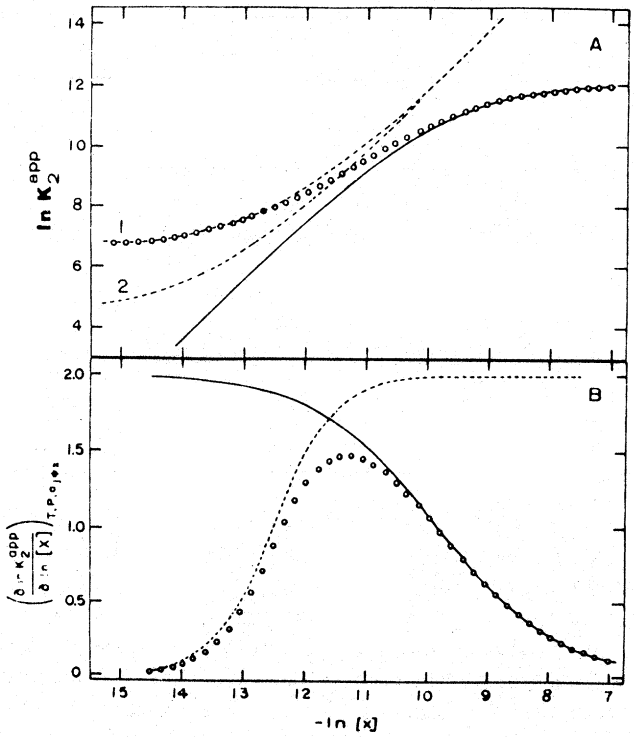

FIG. 15. Wyman plots of the apparent dimerization constant for the ligand-mediated, ligand-facilitated, and ligand-mediated plus facilitated mechanisms of self-association. (A) $\ln K_2^{app}$ versus ln[X]. The solid line is for ligand-mediated self-association, where $k_1 = 1.8 \times 10^4\ M^{-1}$ and $k_2 = 1.8 \times 10^5\ M^{-1}$. The two dashed lines are for ligand-facilitated self-association, where the intrinsic equilibrium constants used are (1) $k_3 = 2.7 \times 10^5\ M^{-1}$ and $k_4 = 8 \times 10^2\ M^{-1}$, and (2) $k_3 = 8.5 \times 10^5\ M^{-1}$ and $k_4 = 80\ M^{-1}$. The open circles are for the ligand-mediated plus facilitated mechanism of self-association where $k_1 = 1.8 \times 10^4\ M^{-1}$, $k_2 = 1.8 \times 10^5\ M^{-1}$, $k_3 = 2.7 \times 10^5\ M^{-1}$, and $k_4 = 8 \times 10^2\ M^{-1}$. (B) $(\partial \ln K_2^{app}/\partial \ln[X])_{T,P,a_j}$ versus ln[X]; the symbols have the same meaning as in (A). (Taken from Ref. 10.)

tive average ligand bindings by the reactant and the product. The Wyman linked function states that $\Delta\bar{X}$, the slope of the above double logarithmic plot, should be equal to the difference between the average ligand bound to the product and the average ligand bound to the reactant. For the above described association mechanisms, these derivatives are listed in the last column of Table II and their values are depicted in Fig. 15B. It is evident that $\Delta\bar{X}$ is dependent on the ligand concentration and the association mechanism. For the ligand-mediated self-association defined above, the slope of the double-logarithm plot at low ligand concentration approaches

two, the stoichiometry of the ligand in the self-association reaction. It approaches zero at saturating ligand concentration. On the other hand, for a ligand-facilitated self-association, the slope approaches zero at low ligand concentration but reaches two at high ligand concentration. For the combined ligand-mediated and facilitated self-association, $\Delta\bar{X}$ approaches zero at both the high and low ligand concentration ends, while, between these two extremes, it reaches a maximal value which is a function of the two ligand binding constants, k_1 and k_3, and is less than two, the ligand stoichiometry in the dimerization reaction. For the cross-linking mechanism of self-association, the Wyman plot shows an initial increase followed by a decrease of ln K_{app} with increasing free ligand concentration. This is because, at high ligand concentration, the ligand binding sites tend to become saturated, which drives the macromolecule to its monomeric state. Thus, by plotting ln K_{app} versus ln[X] and fitting the data with theoretical curves calculated for different association schemes, one can deduce the mechanism of linkage as well as the intrinsic equilibrium constants of the ligand-induced self-association reaction.

The procedure of the data analysis is as follows. One should focus on the apparent association constant of a single association step at a time. For an isodesmic type self-association, the conclusions derived from analyzing a single apparent association constant should be applicable to all the association steps with the same association constant. For a given association mechanism, list out all of the macromolecular species stipulated by the mechanism and express the apparent association constant accordingly. This is followed by nonlinear least-squares fitting of the experimentally obtained apparent association constants with the equation. Examples of such a linkage analysis are provided by the calcium and hydronium ion effects on hemocyanin subunit association,[37] and the magnesium-induced and vinblastine-induced tubulin self-associations.[7-10] In order to derive the microscopic equilibrium constants, it is necessary that the apparent association constant be determined over a wide range of ligand concentrations, preferably at least one order of magnitude from both ends of half-saturation, i.e., from one-tenth to 10 times of $1/K_x^{app}$, where K_x^{app} is the apparent ligand binding constant. This is exemplified by the vinblastine-induced tubulin self-association shown in Fig. 16A where curve fitting of the Wyman plot provided the microscopic equilibrium constants and indicated that the isodesmic indefinite self-association of tubulin proceeds through a one-ligand-mediated mechanism.[10]

A word of caution is needed regarding the interpretation of the linked function analysis. It is often said that an equilibrium study cannot be used

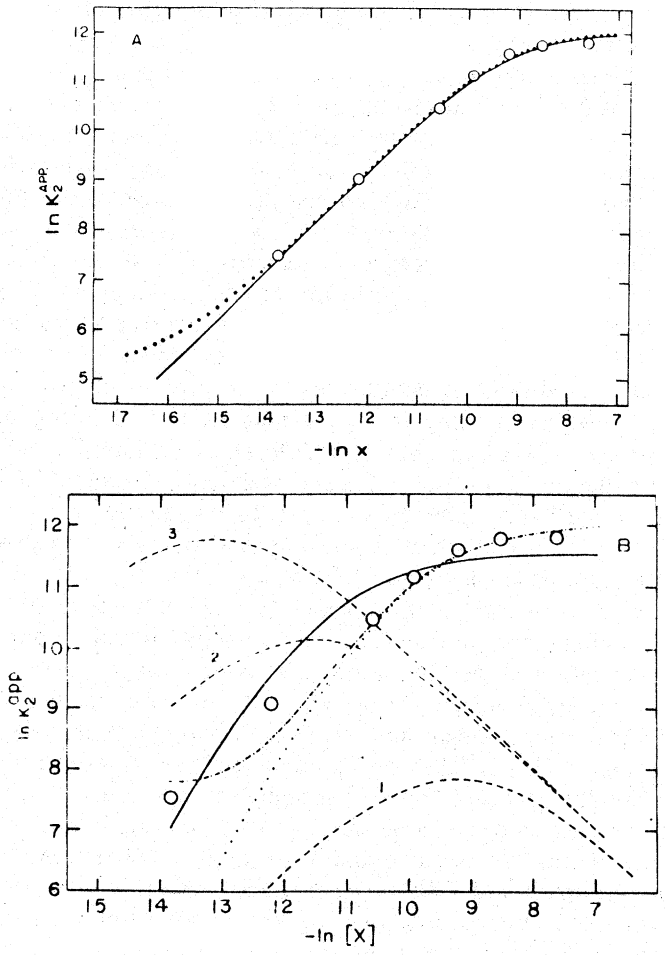

FIG. 16. Wyman plot of the experimental apparent dimerization constants for the vinblastine-induced self-association of tubulin and their least-squares fittings by different reaction mechanisms. The experimental results are depicted by the open circles. (A) Least-squares fittings by one-ligand-mediated mechanism (——) and one-ligand-mediated and facilitated mechanism (···). (B) Least-squares fittings by two-ligand-mediated mechanism at [vinblastine] $\geq 1 \times 10^{-6}$ M (——) and at [vinblastine] $\geq 2.5 \times 10^{-5}$ M, (···) and two-ligand-mediated and facilitated mechanism (---). The dashed lines in (B) are the Wyman plots for self-association via a cross-linking mechanism. The intrinsic equilibrium constants, k_1, used in this case are (1) 1×10^4, (2) 1×10^5, and (3) 5×10^5 M^{-1}. (Taken from Ref. 10.)

to prove a reaction pathway. Indeed, what the Wyman linked function analysis provides is a free energy map of the macromolecular states and the manner in which it is affected by the free ligand concentration. At equilibrium, the distribution of the macromolecules among the various states should follow the Boltzmann equation. This molecular distribution is a static picture and not a dynamic one. It tells nothing about how the macromolecules are converted from one state to another. However, the equilibrium distribution of macromolecule as a function of ligand activity can often be used as evidence to rule out certain reaction pathways. This usage of the linked function is best expressed in the words of J. Wyman[29]: "Although by itself the principle, being thermodynamic, has nothing to say about mechanism, nevertheless it provides a powerful touchstone for exploring the implications of any proposed mechanism as well as for establishing the consistency of underlying observations at a phenomenological level."

Concluding Remarks

In the past two decades, both the theory and methodology of velocity sedimentation have made such significant advances that it has evolved into a powerful tool for the examination of macromolecular self-associations. Computer simulation of velocity sedimentation boundaries has contributed significantly to this and it should continue to guide future developments. On the theoretical front, our knowledge is slowly gaining ground in the area of predicting the sedimentation coefficient and hydrodynamic nonideality based on the size and shape of a macromolecule. It is evident that further development in this area is needed in order to strengthen the technique to allow fully quantitative characterization of macromolecular associations. In this context, it is certain that the potential of the velocity sedimentation technique can be greatly enhanced by using it in conjunction with other physical methods, such as electron microscopy, light scattering, and X-ray diffraction.